DSTO

Numerical Modelling of Shock Wave and Pressure Pulse Generation by Underwater Explosions

John M. Brett

DSTO-TR-0677

] APPROVED FOR PUBLIC RELEASE

DEPARTMENT ◆ OF DEFENCE

DEFENCE SCIENCE AND TECHNOLOGY ORGANISATION

Numerical Modelling of Shock Wave and Pressure Pulse Generation by Underwater Explosions.

John M. Brett

Maritime Platforms Division
Aeronautical and Maritime Research Laboratory

DSTO-TR-0677

ABSTRACT

The continuing development of multi-purpose finite element analysis (FEA) codes permits their application to provide new and penetrating insights into the difficult subject of underwater explosive effects and the coupled response of nearby structures. In this paper we investigate the use of one such code (DYNA2D) to model the physical processes associated with an underwater explosion. We compute models covering a range in explosive masses and depths of detonation. The models are shown to simulate much of the important physics of an underwater explosion including: explosive detonation, shock wave generation and transmission, bubble pulsation and the generation of bubble pulse pressure waves. The model results are compared to published experimental data for key features of an underwater explosion such as bubble periods, maximum bubble radii and characteristics of the shock and bubble pressure waves. The good quantitative agreement found for many of these features demonstrates that FEA codes can be used to model important aspects of an underwater explosion. Nevertheless a number of limitations are identified, the most serious of which is the absence of some important energy loss mechanisms associated with bubble collapse.

RELEASE LIMITATION

Approved for public release

DEPARTMENT OF DEFENCE

DEFENCE SCIENCE AND TECHNOLOGY ORGANISATION

Published by

DSTO Aeronautical and Maritime Research Laboratory
PO Box 4331
Melbourne Victoria 3001 Australia

Telephone: (03) 9626 7000
Fax: (03) 9626 7999

AR-010-558
June 1998

APPROVED FOR PUBLIC RELEASE

Numerical Modelling of Shock Wave and Pressure Pulse Generation by Underwater Explosions.

Executive Summary

DSTO provides valuable advice and support to the RAN in a number of areas connected with the vulnerability of ships and submarines to underwater weapons. In order to offer such advice it requires a thorough understanding of the underwater damage process and the capability to predict damage for specified weapon-target engagements. A key requirement in this area of defence science is the development of a modelling capability for underwater explosions and their effects on nearby vessels.

By virtue of their ability to couple fluid motions and target deformations finite element analysis (FEA) codes are potentially a valuable tool for studies of damage from underwater explosive events. However, before such codes can be confidently applied to damage prediction it must be demonstrated that they can reliably simulate experimental data for the underwater explosion itself. As a first step in this process of verification the FEA code DYNA2D has been used to model the relatively simple case of an isolated underwater explosion producing a spherically symmetric pulsating bubble.

The models presented in this report were able to simulate much of the important physics of an underwater explosion including the generation and propagation of shock waves, pulsation of the bubble of detonation product gases, and the generation and propagation of bubble pulse pressure waves produced by bubble collapse. Comparison to experimental results showed that the models satisfactorily reproduced a number of important characteristics of the explosion. However other characteristics were poorly reproduced and this can be attributed to both limitations of the FEA code employed and the simplifying but restrictive model assumptions. It is suggested that the most significant of these limiting assumptions is that of symmetric pulsation which precludes the loss of energy associated with asymmetric bubble collapse - in particular the formation of a water jet.

Removal of these restrictions can be expected to improve the realism of the models but in practice a more sophisticated implementation of the DYNA code will be needed to accommodate the excessive mesh distortion produced from asymmetric bubble collapse. This will be addressed in future work but for the moment the modelling approach presented in this report can be applied to studies of target damage dominated by loading from the shock wave and the first (strongest) bubble pulse pressure wave.

Authors

John M. Brett
Maritime Platforms Division

John Brett was awarded a Phd in Astrophysics from the Australian National University in 1988 following which he spent five years engaged in postdoctoral research at universities in England, Sweden and Australia. He joined the Maritime Platforms Division (then SSMD) of AMRL in 1993 and since then has been researching underwater explosive damage effects and associated aspects of submarine vulnerability.

Contents

1. Introduction

The underwater explosion produced by the detonation of a submerged high explosive device poses a serious threat to the integrity of any nearby structure. Such an event consists of a complicated sequence of energetic physical processes, but from the point of view of damage to structures it can be simplified to the generation of pressure waves (acoustic and shock) and the fluid flows produced by the dynamic interaction of the detonation product gases and the surrounding water. Immediately following the completion of the detonation phase an underwater explosion can be conceptualised as a water-bourne shock wave and an expanding bubble of detonation product gases. The shock wave, generated when the detonation wave within the explosive reaches the explosive-water interface, travels out through the water at high speed. The very high pressures associated with the shock wave can inflict considerable damage on any vessel or structure it encounters which is not strong enough to resist this loading. Yielding structures introduce complications into the shock wave loading; rapid deformation of a structure produces tension and resultant cavitation in the adjacent water. Although this cavitated region initially affords some protection against loading from the tail of the incident shock wave , its eventual collapse against the structure is another source of potential damage.

The subsequent development of the bubble and its interaction with the surrounding water produces other phenomena which are also capable of causing considerable damage, particularly if the bubble is formed nearby. Behind the receding shock wave the high pressure gas bubble expands at a much slower rate, pushing back the water as it does so. The momentum acquired by the water causes the bubble to expand well beyond the point at which internal bubble gas pressure and external hydrostatic water pressure are balanced. Consequently when the expansion is finally brought to a halt, the gas pressure of the bubble is less than the hydrostatic pressure and the bubble begins to contract, slowly at first but with increasing speed. As in the expansion phase the in-falling water acquires momentum which compresses the bubble to much higher pressures than the surrounding hydrostatic value. Thus when it reaches its minimum diameter the bubble is set to begin a new cycle of expansion and contraction. This pulsational behaviour can repeat a number of times, although energy losses limit the importance of subsequent cycles and the presence of water boundaries can disrupt the bubble.

A number of important damage mechanisms are associated with collapse of the bubble. The rapid compression of the bubble around the time of minimum diameter produces a pressure pulse in the surrounding water. Although the peak magnitude of this pressure pulse is less than that of the shock wave, its duration is longer so that its impulse can be comparable. Another significant damage mechanism occurs if the bubble collapses asymmetrically. This produces a high speed directional flow of water passing through the bubble in the direction of the asymmetry. The hydrostatic pressure gradient associated with increasing water depth produces such a jet directed towards the water surface. The obstruction of water flow due to the presence of a nearby structure also causes asymmetric collapse and the formation of a water jet

directed towards the structure. A useful overview of underwater explosions has been presented by Snay (1957) and for a more detailed account the reader is directed to Cole (1948).

Understanding and being able to model this sequence of events and the associated damage mechanisms has obvious applications in defence science. This important problem has been studied for many years using experimental and theoretical methods and in more recent decades the advent of high speed computers has enabled the problem to be studied using the method of computational modelling. Whilst experimental studies are always to be encouraged, in many cases for reasons of safety and cost, it would be desirable to make damage predictions by means of computer modelling. Individual aspects of an underwater explosion can be modelled with a number of different methods. For example, studies of shock loading alone can be performed economically by loading a target surface with a prescribed pressure profile and the fluid flows associated with bubble collapse have been successfully modelled with the boundary element method (eg Best & Kucera, 1992). However, such segented modelling approaches cannot represent the combined loading of shock and bubble effects which is important for studies of explosions in close proximity to a target. To achieve this we need to model the complete process of detonation, shock wave emission and interaction with the target, followed by bubble development and the associated water flow and bubble collapse events. To model this full range of phenomena and the coupled response of a nearby target, generalised dynamic finite element analysis (FEA) codes appear to be the best approach. It has been shown that such codes can reproduce the basic physical process of an underwater explosion (Mader 1971, Molyneaux et al. 1994, Shin & Chisum, 1996 and Chisum & Shin, 1996) and the qualitative effects of the interaction with an idealised submerged target (Huang & Kiddy 1994). However before these tools can be used for reliable damage predictions we need to demonstrate a convincing quantitative agreement between their predictions and experimental results. Some studies along these lines have been published (eg Brett & Reid, 1995 and Sandusky et al. 1996) but more is needed before we can apply the computer modelling approach with confidence.

As part of a wider vulnerability assessment program for naval vessels we are undertaking both experimental and computational studies of the effect of underwater explosions on submerged and floating structures. Our overall strategy in this program is to use experimental results to validate computational methods which can then be used for further studies not easily accessible to direct experimentation. In this paper we detail the first step in this process, which has been to investigate the ability of FEA codes to reproduce the shock wave and bubble pulse behaviour of an underwater explosion. After first establishing an appropriate specification for the finite element models (grid resolution and structure, boundary constraints etc), we proceed to investigate their physical behaviour. Following this we make a comparison to published experimental data for underwater TNT explosions, focussing on bubble behaviour and the production of shock and pressure waves.

2. Description of Models

For this initial investigation we consider the relatively simple problem of an isolated spherical mass of explosive detonated at great depth with no influence of boundaries such as the sea surface or floor. The presence of boundaries can affect bubble expansion and subject it to the return of reflected pressure waves; the study of such complications is postponed to a later date.

The models were computed with the HYDROSOFT PC version of the non-linear Arbitrary Lagrangian Eulerian (ALE) DYNA2D FEA code (Whirley et al, 1995), together with the MAZE pre-processor (Hallquist, 1983) and ORION post-processor (Hallquist & Levatin, 1985). The inclusion of the ALE feature in DYNA allows it to model problems involving severe mesh distortion whilst still retaining the advantages of modelling any structure with the Lagrangian method. This new feature should therefore be very applicable to modelling the coupled fluid structure interaction involved in a underwater explosion near a submerged structure. It must be pointed out at the onset that at the time of this study the DYNA codes available are not able to adequately model the process of asymmetric bubble collapse and consequently cannot model the generation of water jets. This will require a more sophisticated ALE feature which may become available in the near future. To avoid this problem we made the further assumption that hydrostatic pressure is constant throughout the range of depths encompassed by the model thereby producing spherically symmetric bubble expansion and collapse. This assumption is only realistic where the maximum bubble size is small compared to the pressure gradient and so the models are most relevant to the detonation of smaller charge masses at larger depths rather than for larger charges at shallower depths.

All computations were performed using a 166Mhz Pentium PC with which a typical model required about 80 mins of CPU time to run.

2.1 Model Parameters

Our simplified underwater explosive event can be fully specified by the mass and type of explosive, and the depth of detonation. Because we deal exclusively with TNT as the explosive type, the mass and depth of detonation are the only input parameters to our models. In the following we label a model with the parameter pair (W, Z) where W is the weight of explosive in kg and Z is the water depth in meters.

2.2 Grid Construction

The initial geometry of the models which employed axisymmetry about the y axis is shown in Figure 1. Each model was constructed as spherical shells of water surrounding a central sphere of explosive which was composed of 600 elements. Immediately next to the explosive was an inner shell of water with a radius of about 3

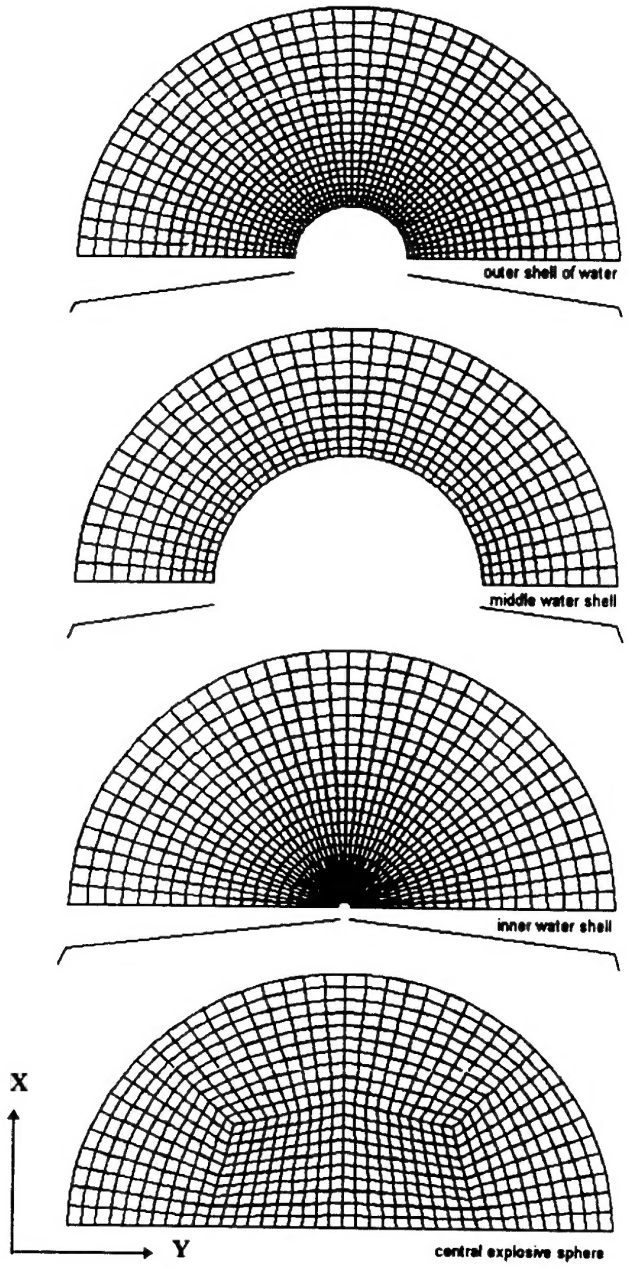

Figure 1. Exploded view of grid structure of UNDEX model working from the outermost water shell at the top to the central core of explosive at the bottom. The y axis is an axis of symmetry.

times the expected maximum bubble radius, as calculated from empirical relations for bubble pulsation (eg Swisdak, 1978). This dimension was chosen to allow the bubble to expand without excessive compression of the water elements in the radial direction. Immediately surrounding this inner shell was another shell of water elements of twice its diameter. Different model grid resolutions were investigated (see below) but satisfactory results were derived for models with the inner shell divided into 20 elements in the radial direction and 40 elements in the circumferencial direction, and the outer shell divided into 10 elements radially and 40 elements in the circumferencial direction. In the following this is referred to as our standard resolution. The central sphere of explosive and these two shells of water material comprised the central or core part of the models. This was found to be sufficient to reproduce the mechanism of bubble pulsation but for reasons described below (section 2.3), an adequate quantitative simulation compared to observed bubble behaviour required the addition of a further outer shell of water. The resolution of this outermost shell was 20 elements in the radial direction and 40 elements in the circumferencial direction.

Following detonation, the expansion of the central explosive causes excessive distortion of the surrounding shells of water elements as their radial dimensions are reduced and circumferential dimension are stretched. The ALE option was employed to assist in handling this problem for the water elements contained within the core part of the models, but because it is unable to move boundary nodes it was necessary to perform regular rezoning of the water boundary nodes on the central axis of symmetry. This was performed using the automatic rezoning facility in DYNA. Without this additional rezoning procedure, the models would not run satisfactorily.

2.3 Boundary Conditions & Restraints

A key feature of an underwater explosion is the maximum size of the bubble. Expansion of the bubble is influenced by hydrostatic pressure and inertia of the surrounding water and so the models must include this to give reasonable results for bubble growth. The variation of pressure (P) with water depth (Z) is given by the equation of hydrostatic equilibrium

$$dP = g\rho(Z)dZ \qquad (1)$$

where ρ is the density of the water and g is as usual the gravitational acceleration. For sea water with a density of 1030 kgm^{-3} this equation is equivalent to an increase of 1 atm pressure per 10 m increase in depth. Using DYNA the hydrostatic stresses within a material caused by an overburden can be initialised with a density vs depth relation. To make use of this feature to set initial hydrostatic water pressure, a ρ vs Z relation was derived as follows. From the definition of bulk modulus

$$B = dP / (dV / V)$$

for pressure P and volume V, and its relationship to the speed of sound v

$$B = v^2 \rho$$

we obtain a relation between P and ρ,

$$dP = v^2 d\rho$$

which can be combined with Equation 1 to derive the required relation between depth and density as

$$\frac{d\rho}{\rho} = \frac{g}{v^2} dZ$$

The slight dependence of ρ on υ as well as on Z was overcome by assuming a constant speed of sound to give a starting estimate of the required value of ρ for a given value of Z. DYNA was then run to fine- tune the water density to produce the water pressure for a given depth as given by Equation 1.

Because of the importance of inertia of the water in determining bubble behaviour, the outer boundary of the model required special attention. One possible option for simulating the bulk inertia of the water would be to make use of a suitably positioned external rigid boundary but this would reflect the shock wave (and bubble pulse waves) back into the model which would impact on the bubble surface and affect its subsequent development. To avoid this problem we were forced to include a sufficient amount of surrounding water in the models to provide enough inertia to simulate a free field environment, the required extent of this was found by experiment (see section 3.1). The outermost edge of each model was free to move and was made a non-reflecting boundary to prevent the unwanted reflection of tension waves.

2.4 Material Models

The material models for water and TNT were taken from the DYNA materials library but for completeness the details are presented here. The TNT detonation process follows that of Giroux (1973) using a detonation velocity of 6930 ms^{-1} and a Chapman-Jouget pressure of 21 GPa. Development of the detonation product gases is modelled with the standard JWL equation of state (Dobratz, 1981) for which the pressure within the detonation product gases is given by

$$P = A\left(1 - \frac{\omega}{R_1 V}\right)e^{-R_1 V} + B\left(1 - \frac{\omega}{R_2 V}\right)e^{-R_2 V} + \frac{\omega E}{V}$$

in which V is the ratio of the volumes of detonation products to that of the undetonated explosive, E is the detonation energy per unit volume and A, B, R_1, R_2 and ω are fitting coefficients.

Water was modelled as a compressible fluid with the Gruneisen equation of state, following Woodruff (1973), whereby the pressure (P) is defined as

$$P = \frac{\rho_0 C^2 \mu \left[1 + \left(1 - \frac{\gamma_0}{2} \right) \mu - \frac{a}{2} \mu^2 \right]}{\left[1 - (S_1 - 1)\mu - S_2 \frac{\mu^2}{\mu + 1} - S_3 \frac{\mu^3}{(\mu + 1)^2} \right]^2} + (\gamma_0 + a\mu) E$$

for compressed materials ($\mu>0$) and as

$$P = \rho_0 C^2 \mu + (\gamma_0 + a\mu) E$$

for expanded materials ($\mu<0$) where the excess compression μ is defined in terms of current density ρ and initial density ρ_0 by

$$\mu = \frac{\rho}{\rho_0} - 1$$

In this formulation γ_0 is the Gruneisen gamma, a is its first order volume correction, and C, S_1, S_2, S_3 are the intercept and three slope coefficients of the shock velocity vs particle velocity curve respectively. All material parameters and constants together with their values as specified in the DYNA materials library (converted to SI units) are listed in Table 1.

The DYNA fluid model includes a pressure cut-off or maximum tensile strength for water which was set to -3 atm; the water is presumed to cavitate below this threshold. In principle this low cavitation limit would allow unrealistically strong tension in the water, but the absence of any yielding reflecting surfaces in the models makes its actual value unimportant; altering it to a more realistic -1 atm produced only minimal changes in bubble behaviour.

Table 1. Material Parameters and Constants

Symbol	Meaning	Value
TNT		
ρ	density	1630kgm^{-3}
D	detonation velocity	6930 ms^{-1}
P_{cj}	Chapman-Jouget pressure	21 Gpa
A	fitting coefficient	371.2 GPa
B	"	3.23 GPa
R_1	"	4.150
R_2	"	0.950
ω	"	0.30
E_0	detonation energy / unit volume	7 GPa
H_2O		
ρ	density	1000 kgm^{-3}
C	speed of sound	1480 ms^{-1}
S_1	fitting coefficient	2.56
S_2	"	-1.986
S_3	"	0.227
γ_0	gruneisen coefficient	0.50
a	volume correction coefficient	0.0
E_0	initial internal energy / unit volume	0.0

3. Numerical Results

In this section we present a strictly numerical analysis of the models, investigating physical processes, model sensitivities and internal self consistency. Key attributes of an underwater explosion are the maximum diameter (A_{max}) and period (T_{bubble}) of the first bubble pulsation; accordingly we make substantial use of these attributes in the following analysis.

3.1 Grid Size Dependency

As explained above it was necessary to surround the core part of each model with additional water to provide sufficient inertia to adequately model the behaviour of the bubble. The effect of increasing the mass of the surrounding water was to increase both the period of oscillation and the maximum bubble radius, which demonstrates the importance of water inertia in bubble dynamics. The extent of water required to

adequately model bubble pulsation was found by increasing its diameter until the change in bubble size and period was not significantly affected by further increases in diameter. From tests conducted with a (1.0,100.0) model of standard resolution it was found that the addition of an outer shell of 5 times the diameter of the core model (thirty times the expected maximum bubble radius) resulted in changes of 16 % in A_{max} and T_{bubble}. Doubling the diameter of the outer shell again produced only small additional changes. Consequently all models were computed with an outer shell of diameter 5 times that of the inner core.

3.2 Model Resolution Dependency

It is well known that the resolution of an FEA model can affect its behaviour and so a test of the dependency of the key bubble parameters (A_{max} and T_{bubble}) on the resolution of the model grid is appropriate. A (1.0,100) model was computed at a number of different grid resolutions, slowly increasing the number of elements in key zones and assessing the change in A_{max} and T_{bubble} , with the objective of finding a limit beyond which further increases in resolution produced little further change. During this process it was found that overall increases in resolution soon exceeded the storage capacity of DYNA, requiring a more selective refinement of the grid. Due to the radial symmetry of the problem it was possible to limit these tests to refinements in radial resolution only. Furthermore by experimentation it was found that the key model zones affecting A_{max} and T_{bubble} were the two inner shells of water, changes in resolution of the explosive and the outer water shell having little effect. Figure 2 shows the change in T_{bubble} against the total number of radial elements in the two inner water shells. The tendency to a limit can clearly be seen indicating that further increases in resolution would be unprofitable.

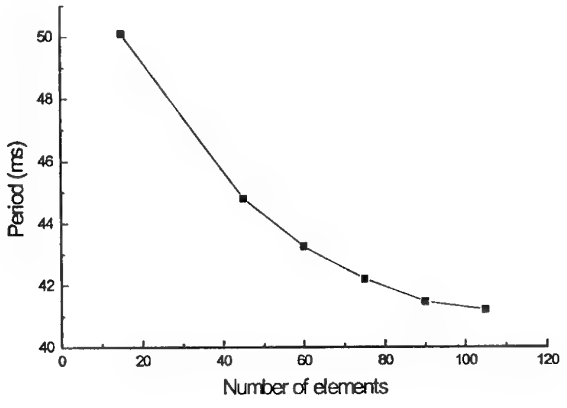

Figure 2. Grid resolution sensitivity: dependence of the computed first bubble period upon the number of elements in the radial direction within the inner water shells.

3.3 Physical Behaviour

In this section we wish to explore the general physical behaviour of our models and for this purpose we analyse our standard resolution (1.0,100.0) model. A careful comparison to experimental data will be made in the next section using higher resolution models with parameters chosen to match experimental conditions.

Motion of the bubble surface can be studied in the plots of radius and velocity magnitude ($\sqrt{(v_x^2 + v_y^2)}$) for several selected surface elements and nodes of the TNT material, presented in Figures 3a and 3b. The pulsational behaviour of the bubble is clearly seen with the bubble undergoing 2.5 pulsations within the 100 ms following detonation. Notable features of the pulsation are the sharp changes in velocity around times of minimum diameter and the extended period of low velocity around times of maximum diameter. The particularly high but brief initial velocity peak is caused by passage of the detonation wave. The small amplitude and high frequency modulations (of period 2 ms at t=5 ms) in the velocity plot can be traced to repeated reflections, within the bubble, of the shock wave off the gas - water interface. This feature is probably artificial because physical processes within a real bubble such as radiative opacity effects, as well as departures from perfect symmetry and homogeneity will lead to dissipation of the internally reflected waves.

The maximum diameter of the bubble decreases with time, and to a lesser extent, the minimum diameter increases. By equating it to the work done during expansion against the hydrostatic pressure the stored potential energy of the bubble (E_p) at a given bubble maximum can be calculated from

$$E_p = \frac{4}{3}\pi R^3{}_{max} P_0 \qquad (2)$$

where P_0 is the hydrostatic pressure and R_{max} is the maximum bubble radius of the pulsation in question. From the ratio of R_{max} for the 1st and 2nd bubble pulsations shown in Figure 3a we can estimate that the energy stored in the bubble on its second expansion is only 60% of that stored in the 1st expansion. Clearly this decrease in R_{max} requires the loss of energy from the bubble and *one* mechanism by which this can be achieved is the emission of pressure waves into the surrounding water.

Figure 3c shows the variation of pressure at the bubble surface caused initially by passage of the detonation wave and then by subsequent bubble collapse events. As expected the shock wave produces a sharp rise in pressure to the value of the specified TNT Chapman-Jouget pressure of 21 Gpa. The rapid contraction around times of minimum radius produces pressure maxima of lower magnitude. It is interesting to note that for most of the time the internal gas pressure of the bubble is below the hydrostatic value, which graphically demonstrates the role of water inertia, as opposed to pressure imbalances, in bubble pulsation.

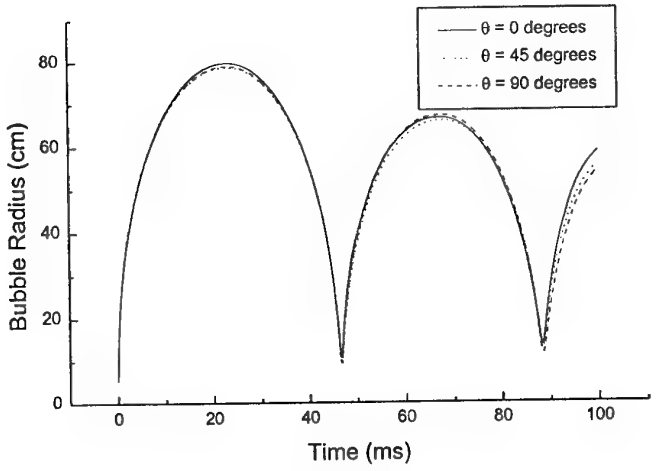

Figure 3a. Radius of selected surface nodes at interface between water and TNT materials. Node positions at the specified angles as measured from the y axis.

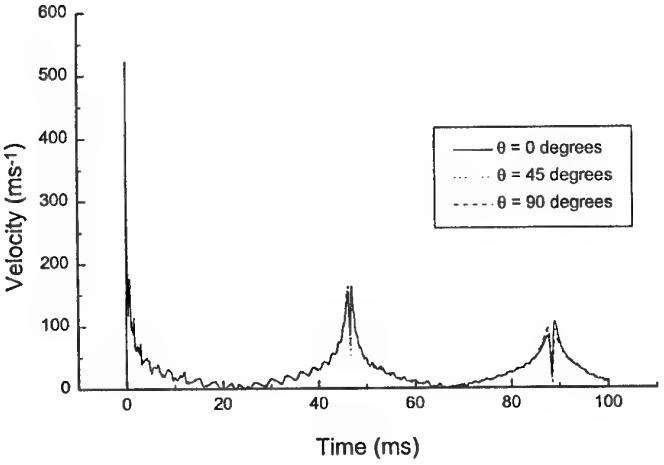

Figure 3b. Velocity magnitude of TNT surface elements corresponding to nodes of Figure 3a. Element positions at the specified angles as measured from the y axis.

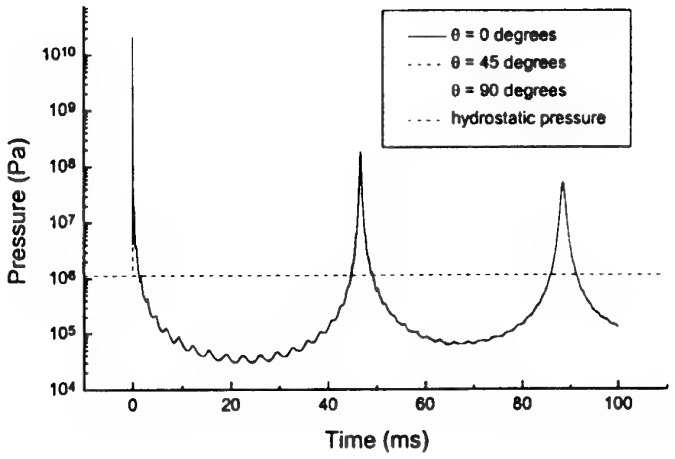

Figure 3c. Pressure of selected surface elements of TNT material. Element positions at the specified angles as measured from the y axis.

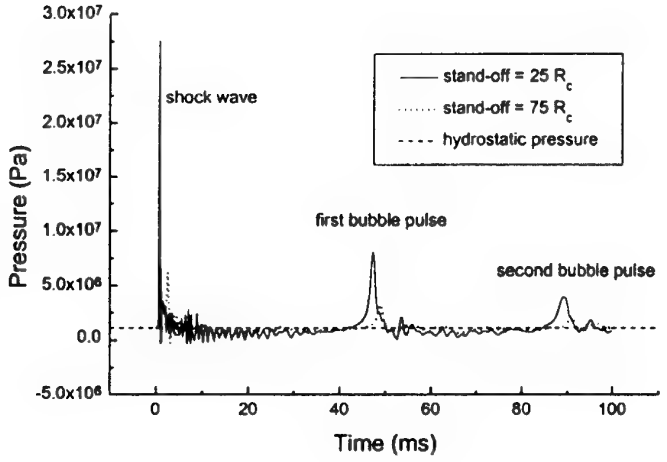

Figure 3d. Time dependence of water pressure measured at stand-offs of 25 R_c and 75 R_c from the centre of the explosive where R_c = initial radius of explosive charge.

The large pressure variations within the bubble are of course transmitted to the water where they are observed as the water shock and bubble pulse pressure waves. The modelling of these phenomena by DYNA is displayed in Figure 3d, where we plot the water pressure at two different distances from the centre of the charge. These model results exhibit a number of features seen in measurements of real underwater explosive events:

i) a classic shock wave profile with a steep shock front and exponential like decay.

ii) broader and symmetrical bubble pulse pressure waves, with amplitude decreasing and width increasing from the first to second pulsations.

iii) lower P_{max} of the bubble pulses compared to the shock wave ($\approx 1/4$) but comparable impulse.

iv) an extensive period (8 ms to 42 ms) around the time of maximum bubble radius during which time the water pressure drops below the hydrostatic value.

This general correlation with real events implies that DYNA is able to simulate much of the important physics involved in an underwater explosion.

As was mentioned above the energy lost during pulsation of the bubble can be calculated from Equation 2. In the models presented here this energy loss can only come from the emission of bubble pulse pressure waves. As will be shown in the following comparison to observations, this limitation presents a problem for the models but for the moment it allows a check on their self consistency. Following the paper of Arons and Yennie (1948), the flux (F) and energy (E) radiated over the time interval t_1 to t_2 can be calculated from measurements of pressure at a stand-off of R from the explosive by

$$F = \frac{1}{\rho_0 C_0} \int_{t_1}^{t_2} (P - P_0) dt \tag{3}$$

$$E = 4\pi R^2 F \tag{4}$$

where ρ_0 , C_0 and P_0 are the undisturbed density, speed of sound and pressure for water. Evaluated over the interval between the times of first and second bubble maximum radii (t_1 = 23 ms, t_2 = 67 ms), at a stand-off of 25 charge diameters (1.32 m), Equations 3 and 4 yield a radiated energy of 0.88 MJ. Evaluation of the change in bubble potential energy from the first to second bubble maxima (via Equation 2) yields a value of 0.89 MJ. Clearly the models are quite self consistent in their treatment of energy losses during bubble pulsation

4. Comparison to Experimental Data

Clearly the most important attribute of any numerical model is how well it can reproduce the behaviour of the real system that it seeks to represent. To test the ability of DYNA to quantitatively model underwater explosions we present a comparison to detailed observations of bubble radius and water pressure measurements of two

individual observed events. This is followed by a more condensed assessment of the ability to reproduce the charge weight and water depth dependencies of key characteristics of underwater explosions. For these comparisons we employ models with the largest possible radial grid resolution of 125 elements within the water material.

4.1 Detailed Comparisons

Experimental measurements of underwater explosive effects have been carried out for a number of years and some of the most accessible results (particularly for TNT) are found in papers published shortly after the second world war. We have selected two examples of this data for detailed comparison to our models: the experiments of Swift and Decius (1950) on bubble radii and the pressure data for deep TNT explosions compiled by Arrons & Yennie (1948).

4.1.1 Bubble Behaviour

Swift and Decius (1950) provide measurements of the bubble radius and period for experiments conducted for a number of charge sizes and detonation depths. Particularly useful for our purpose is their graph of the time variation of bubble radius for a 0.3 kg charge detonated at a depth of 300 ft (91.46 m). This depth should be sufficient to prevent the bubble sensing the water surface boundary and prevent significant interference from reflected pressure waves - as is assumed in our models. We have modelled this experiment with a (0.30,91.46) model and the comparison between predicted and experimental bubble radii is presented in Figure 4. It is apparent from this figure that the radii agree very well for the first pulsation of the bubble but for subsequent pulsations the agreement is very poor, with the model predicting maximum diameters which are too large and periods which are consequently too long.

This discrepancy indicates that too much energy is stored in the bubble at the beginning of the second and subsequent pulsations and explanations for this are not difficult to find. A real pulsing bubble can lose energy by a number of mechanisms, including radiation of pressure waves, turbulence of the water, loss of bubble gases at the water interface, and heat loss from the high temperature bubble gases. In contrast DYNA can only reproduce those mechanisms that are associated with dynamic effects between adjacent elements. Furthermore a primary cause of water turbulence is asymmetric bubble collapse, so that our model restriction to symmetric pulsation precludes energy loss by this mechanism. Although in principle DYNA can include some of the processes involved in asymmetric collapse, practically a Eulerian or more sophisticated ALE technique will be required. Thus of the possible bubble energy loss mechanisms our models can only include the energy lost by the emission of pressure waves and as a result the bubble retains too much energy after the first bubble collapse. From the very good agreement for the first pulsation maximum diameter, we can infer that most of the additional energy losses occur during the collapse phase

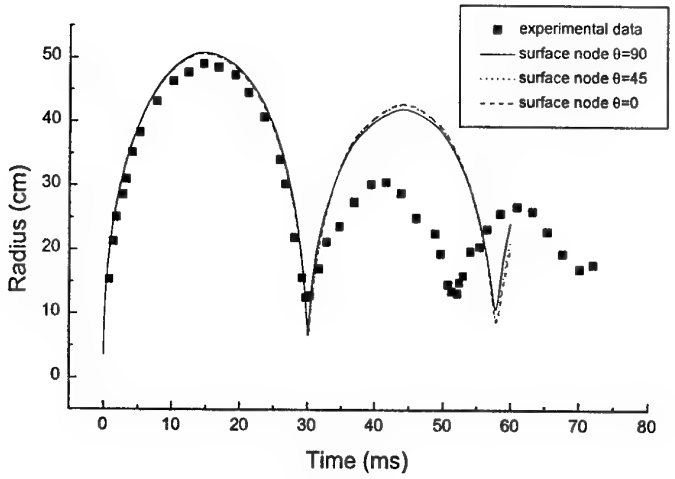

Figure 4. Comparison of computed and experimental bubble radius produced by detonation of 300 g of TNT at a water depth of 91.5 m (300 ft). Experimental data taken from Swift & Decius (1950). Model node positions at the specified angles as measured from the y axis

which may suggest that energy losses associated with asymmetric bubble collapse dominates this. The energy loss not taken into account in the models can be quantified by use of Equation 2 together with the computed and observed values of maximum bubble radius for the first and second pulsations as read from Figure 4. For the observed bubble pulsation the change in maximum radii yields an energy loss of 0.38 MJ, whereas the DYNA calculation predicts an energy loss of only 0.23 MJ - a shortfall of 0.15 MJ. It has been shown above that the loss of potential energy in the models occurs by the emission of bubble pulse pressure waves. Provided it can be shown that the models adequately reproduce the observed bubble pulse pressure wave (see the next section for support of this) then the comparison of Figure 4 indicates that only 60% of the total energy lost by the bubble during the 1st collapse phase is due to the emission of pressure waves, with the rest being presumably by the mechanisms discussed above.

Although the failure to predict bubble behaviour past the first pulsation is disappointing, it should be remembered that this first pulsation is the most energetic and therefore will be the source of the strongest bubble related damage effects. This point is discussed further in the next section.

4.1.2 Shock and Pressure Waves

Arrons and Yennie (1947) provide composite pressure time curves generated from a number of separate measurements of pressure arising from the detonation of 0.5, 2.5 and 12 lb charges at a depth of 250 ft. From this data we have reconstituted a pressure time curve for a 2.5 lb (1.13 kg) charge detonated at a depth of 500 feet (152.4 m). The comparison of this data to results from a (1.13,152.4) model is presented in Figure 5 which, for ease of analysis, has been broken up into separate time intervals containing the shock wave and first and second bubble pulse pressure waves.

For the shock wave we can see that although the initial decay from peak magnitude, and the tail of the computed shock wave matches the observations well, the predicted peak magnitude is only 70% of the experimental value. This discrepancy can be attributed to the difficulty of representing the nearly discontinuous shock front with a model of limited spatial resolution, the front being smeared out over a few computational cells. Shock fronts are better treated by codes incorporating front-trackers or adaptive gridding. In terms of impulse however the comparison is much better; values computed over the positive portion (ie $P > P_o$) of the model and experimental shock waves agree to within 2%. This fact has significance for studies of target damage because in many cases the impulse (rather than the peak magnitude) of the applied load is the major determinant of target deformation.

The absence of a shock front to bubble pulse pressure waves make them more amenable to modelling with an FEA code and Figure 5b shows that DYNA has adequately modelled the first bubble pulse, apart from a small discrepancy in the time of arrival. The impulses of the model and experimental bubble pulses are also in acceptable agreement differing by less than 15%. Given the success displayed in the preceding section in modelling A_{max} and T_{bubble} this success in modelling the 1st bubble pulse should come as no surprise. Likewise given our problems in modelling the bubble behaviour for subsequent bubble pulsations, we cannot expect to successfully model the second bubble pulse pressure waves and Figure 5c clearly shows our failure to do so. As discussed above the model reaches too large a diameter on its second expansion, storing too much potential energy and consequently creating too strong a pressure wave upon its collapse.

This comparison indicates that DYNA can be successfully used to model the pressure loading associated with the shock wave and first bubble pulse. Those caused by subsequent bubble pulsation cannot be successfully modelled. However these pressure loadings are considerably less significant so provided bubble migration affects are not important it should be possible to apply DYNA to model the major sources of pressure wave damage arising from an underwater explosion.

4.2 Charge Size and Depth Dependency

A valid concern which can be raised when conclusions are drawn from limited comparisons between model and experimental results is that the model has been tuned

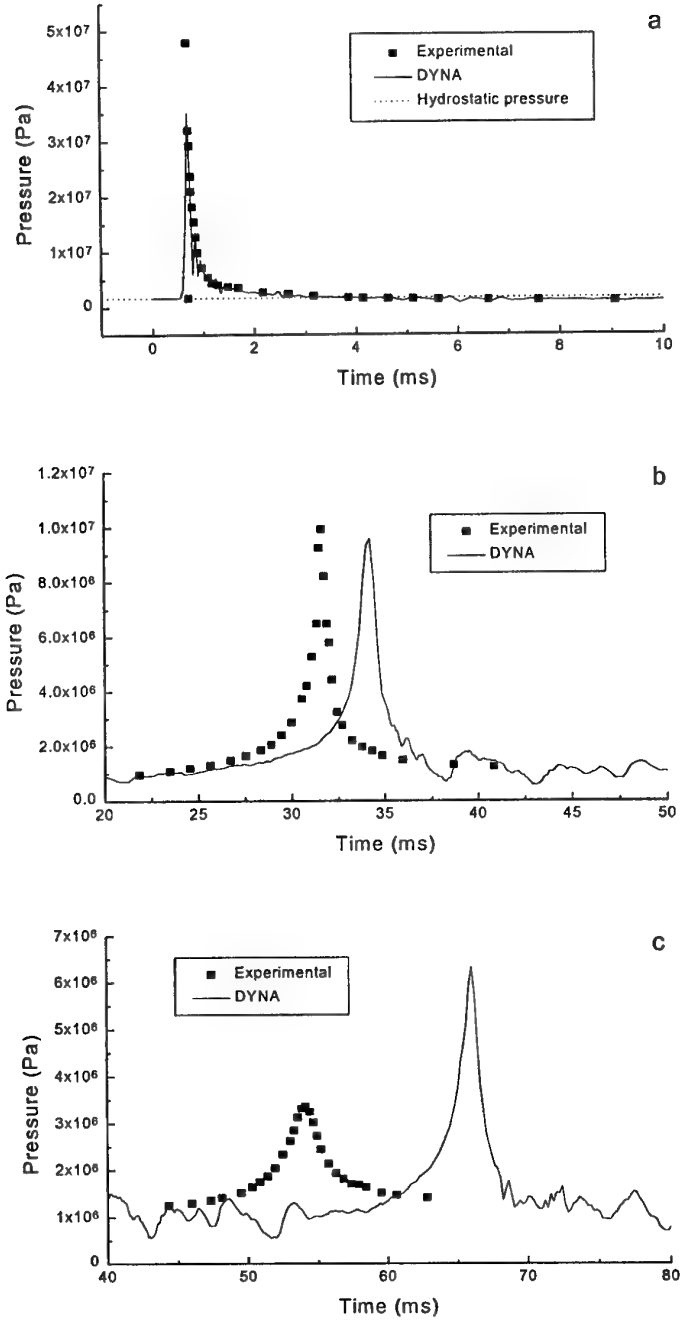

Figure 5. Comparison of experimental and computed pressures for a) shock wave b) first bubble pulse and c) second bubble pulse, from detonation of 1.13 kg (2.5 lbs) of TNT at a depth of 152.4 m (500 ft). Experimental data taken from Arons & Yennie (1948).

to provide the best possible match. Although we have made no attempt to tune the models used in the comparisons just presented we proceed to demonstrate a more extensive comparison for underwater explosions covering a range of depths of detonation (Z) and charge weights (W). For this purpose we have computed models at five depths (100 m, 250 m, 500 m, 750 m and 1000 m) for a fixed charge size of 1 kg, and for four charge weights (0.1 kg, 1 kg, 10 kg and 100 kg) at a fixed depth of 100 m. It has been shown above that the models can only be expected to match features of the shock wave and the first bubble pulsation. For this reason and with the objective of succintness we limit the comparison to values of A_{max} , T_{bubble} and the peak magnitude and impulse of the shock wave and first bubble pulse pressure wave.

To conduct the comparison we require experimental data covering a large range in water depth and charge weight. Measurements of A_{max} and T_{bubble} are in principle relatively simple, being single valued quantities for a given event. Numerous experimental studies (see Cole, 1948) have shown that the dependence of A_{max} and T_{bubble} on water depth and charge weight can be reproduced very well with equations of the form

$$T_{bubble} = K\frac{W^{1/3}}{(Z+10)^{5/6}}$$

and

$$A_{\max} = J\frac{W^{1/3}}{(Z+10)^{1/3}}$$

for metric values of the variables as defined before and the constants K and J being specific for a given explosive type. For comparison to our model results we adopt the values of K = 2.11 $sm^{5/6}kg^{-1/3}$ and J = 3.36 $m^{4/3}kg^{-1/3}$ taken from Swift and Decius (1950). The comparison of model results to data from this source is presented in Figure 6 which shows a convincing reproduction of the experimental dependence of A_{max} and T_{bubble} on both W and Z. This success gives us confidence that DYNA is correctly modelling the major physical processes driving the underwater explosion up until the first bubble collapse.

A comparison to experimental measurements of water pressure is less straightforward because of their dependence on stand-off distance (R) from the explosive as well as Z and W. To ensure self consistency of the experimental data it is desirable to compare to measurements of both shock and pressure waves from the same source. The only published such data for TNT seems to be that of Slifko (1967) who presents results and fitting formula for peak magnitude and impulse produced by the detonation of 1 lb, 8 lb and 57 lb (0.45, 3.64, 25.91 kg) charges of TNT at depths in the range 500 - 14000 ft (152.4 - 4268.3 m). The fitting formula are also presented in metric units by Swisdak (1978). Unfortunately the use of this data presents us with some difficulties. Firstly, as is common to most experimental data (for obvious practical reasons), the pressures are measured at relatively large distances from the explosive ($R/W^{1/3}$ > 200 $mkg^{-1/3}$).

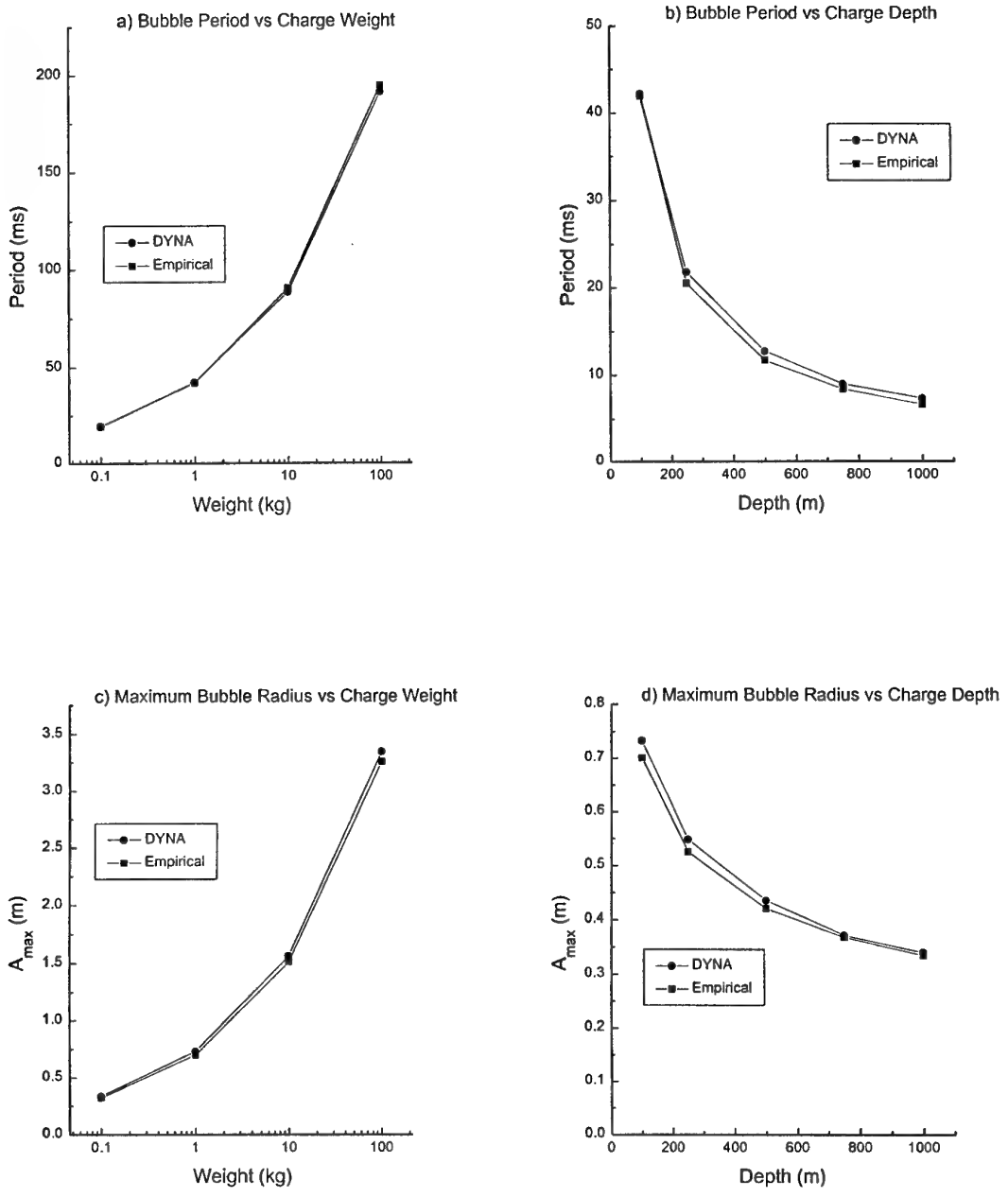

Figure 6. Comparison of experimental and model values of period and maximum bubble radius for first bubble pulsation over ranges in explosive weight and depth of detonation. Experimental values from Swift and Decius (1950).

Including such large stand-offs with reasonable spatial resolution in our DYNA models is impractical. A convenient stand-off for the models is 40 charge radii (R_c), which is well beyond the maximum expansion of the bubble and yet still within the inner well defined shells of the finite element grid, thereby giving the best available spatial resolution. Accordingly to make use of the Slifko data it is necessary to apply the formula at values of $R/W^{1/3}$ outside the range in which they were derived. Other experimental data is available for smaller stand-offs but unfortunately they cover much smaller ranges in W and Z, or measure only one aspect of the underwater explosion. For instance Arons, Slifko and Carter (1948) give peak pressure and impulse measurements for bubble pulses at $R/W^{1/3} = 0.352$ for 8 lb (3.64 kg) charges at two depths of 250 and 500 feet (76.2 and 152.4 m). Coles, Christian, Slifko, Niffenegger and Rogers (1950) present shock wave data covering the range $1.25 < R/W^{1/3} < 25$ and Swisdak (1978) gives similitude equation data for shock waves based on more recent data. Although their restricted coverage makes them less useful for our purpose we can make use of this data to ascertain the validity of extrapolating the Slifko formulae to the smaller stand-offs required by our DYNA models. When allowance is made for some differences between these sources of data, such as explosive charge geometry and integration baselines for impulse, it is found that in general the extrapolated Slifko values agree with the other data to within 10%. This is sufficiently accurate for the objectives of this paper so the extrapolated Slifko formulae are used as the basis for model comparison, making use of the other data only where needed.

4.2.1 The Shock Wave

Figures 7a and 7b show the comparison between predicted and experimental shock wave peak pressures versus Z and W. As was found above in the detailed comparison to experimental pressure results the predicted peak pressures are consistently low which is an unavoidable consequence of the limited model spatial resolution and the associated smearing of the shock front.

The experimental values of peak pressure are constant for both changing Z and W. The constancy with Z is to be expected because pressure is always measured as the excess value above the hydrostatic value. The constancy with W arises from our choice of a constant stand-off of $40R_c$ for measurements of pressure; it is well known that the value of P_{max} obeys the similitude equation

$$P_{\max} = k\left[\frac{W^{1/3}}{R}\right]^{\alpha}$$

for charge weight W and stand-off distance R with constants k and α fitted for a given explosive type (eg. Swisdak 1978). Because we are modelling spherical charges, specifying $W^{1/3}$ is equivalent to specifying R_c and hence a value of R in terms of R_c necessarily leads to a constant P_{max}. The computed values of P_{max} exhibit a slight dependence on both W and Z which is most likely a consequence of the changing spatial resolution. For instance the inner shells of water in the model were constructed

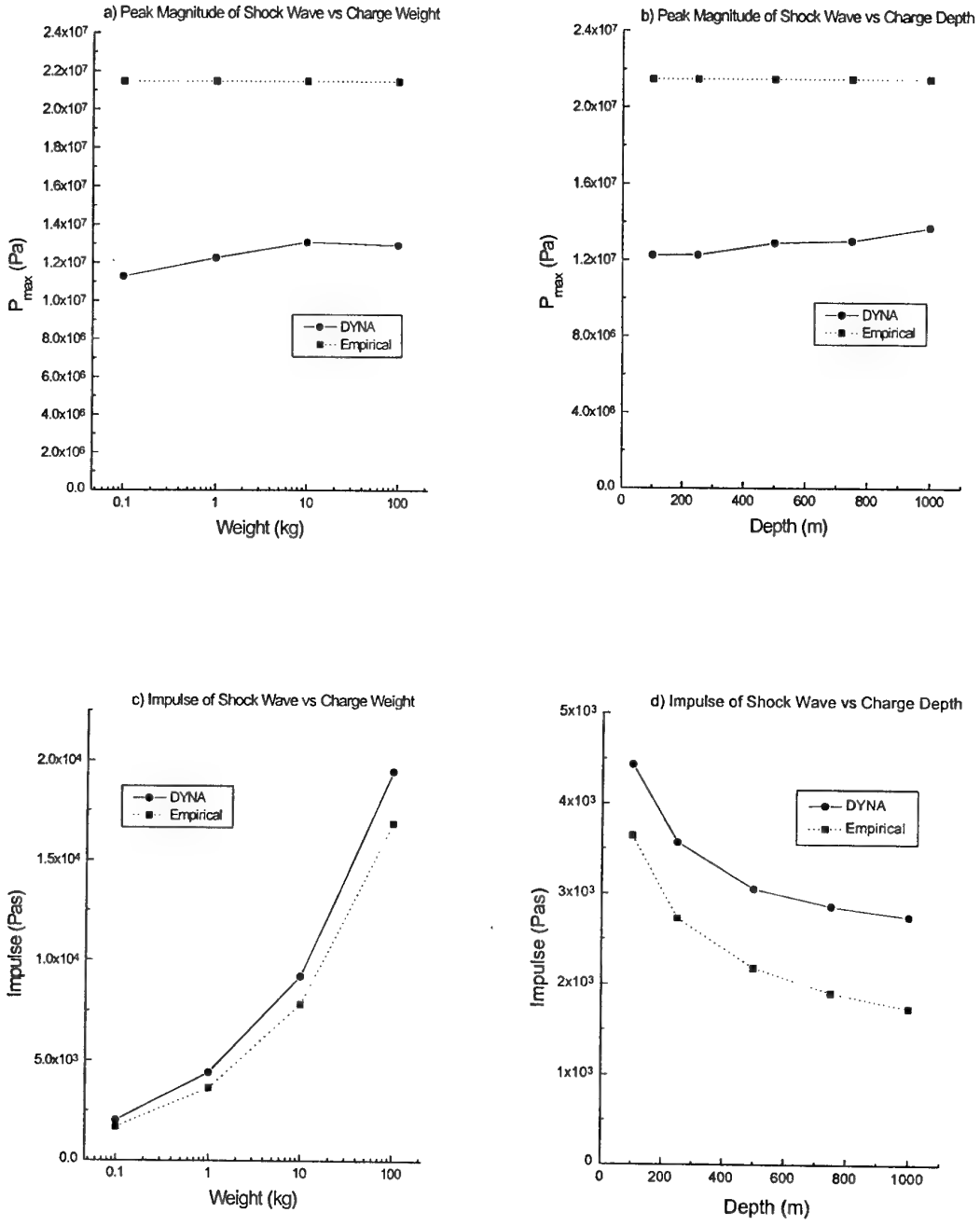

Figure 7. Comparison of experimental and model values of peak magnitude and impulse of the shock wave over ranges in explosive weight (for a fixed detonation depth of 100 m) and depth of detonation (for a fixed charge weight of 1 kg). Experimental values from Slifko (1967).

with a constant number of elements and with a diameter of three times the expected value of A_{max}. Because A_{max} decreases with increasing Z, this produces a smaller element size within the inner water shells and a better definition of the shock wave. The comparison of model values of impulse to the experimental values from Slifko is presented in Figures 7c and 7d which show that DYNA reproduces the trend of experimental dependency on both Z and W, although the offset is in some cases somewhat disappointing. On this point however it should be noted that the magnitude of the experimental data should not be accepted without question. When allowance is made for differences in the integration interval the similitude equations from Swisdak (1978) give an impulse of 3.5 kPas for a 1 kg charge but without any Z dependency. In light of this uncertainty in the experimental data we can be fairly happy with the quality of the fits to it achieved by the models.

4.2.2 The First Bubble Pulse

Figures 8a and 8b indicate a much closer agreement between predicted and experimental values of P_{max} for the bubble pulse than was achieved for the shock wave. As was seen in the earlier detailed comparison to experimental pressure records, this success can be attributed to the smoother and broader profile of the bubble pulse making it more amenable to simulation with a limited resolution FEA model. However, despite the generally better match of gross magnitude for the bubble pulse, the models show predicted dependencies on both Z and W which are not supported by the experimental data. The model dependence on W is not large and is seen only for the largest two masses, so we make no attempt to explain it other than to suggest it may be associated with changing grid resolution effects. That for Z however is much more definite and cannot be explained by such effects. In fact as shown in the figure the model results can be fit fairly well with a $Z^{1/6}$ dependence. Interestingly, Slifko finds such a dependence in his data for Z > 1200m, which suggests that our models are more appropriate for the conditions which exist at such large depths.

As discussed by Cole (1948) a depth dependence of P_{max} is seen for bubble pulsation at shallow depths, this being produced by the action of non-symmetric bubble collapse. Simple argument indicates that the assumption of spherically symmetric pulsation becomes more valid as Z increases, and A_{max} decreases relative to the hydrostatic pressure gradient. For shallow detonations, where A_{max} is larger, the gradient may vary significantly over the fully expanded bubble, causing it to collapse faster at its base thereby inducing significant asymmetry and vertical migration of the bubble. This turbulent motion transfers energy to the surrounding water which is not returned to the bubble during its collapse and consequently the collapse is less energetic generating a broader bubble pulse profile of lower peak magnitude. By this reasoning we expect a depth dependence to be seen in P_{max} for values of Z near the surface. However, it is not likely to be significant at the depths encompassed by the Slifko data set and the observed constancy of P_{max} with depth over the range 100m to 1200 meters indicates that this is indeed the case. Moreover the depth dependence exhibited by the models, which assume spherical pulsation, cannot be caused by this effect. Thus it

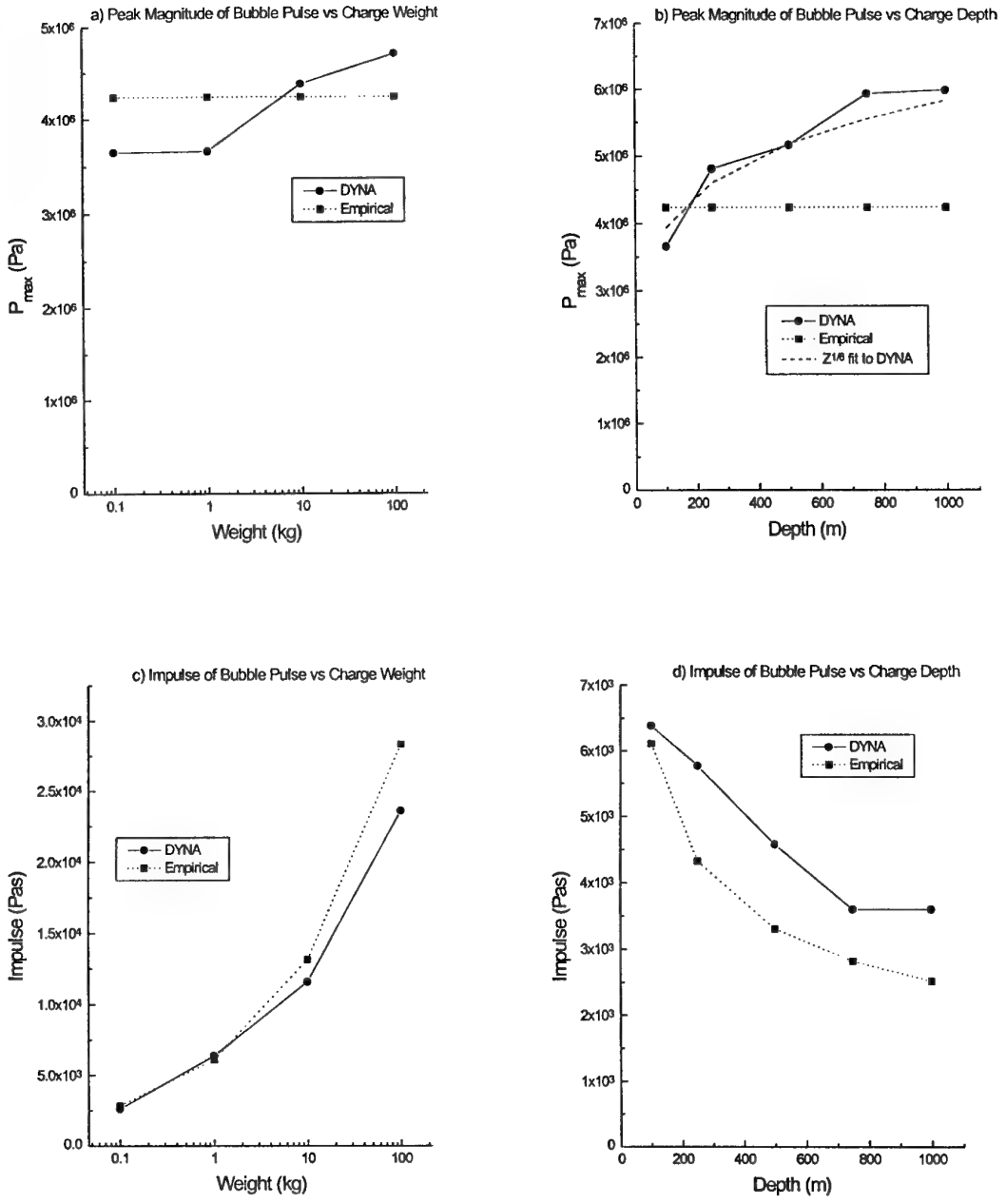

Figure 8. Comparison of experimental and model values of peak magnitude and impulse of the first bubble pulse pressure wave over ranges in explosive weight (for a fixed detonation depth of 100 m) and depth of detonation (for a fixed charge weight of 1 kg). Experimental values from Slifko (1967).

seems some other explanation must be found for the mismatch between the models and observations and in particular the fact that the $Z^{1/6}$ dependence predicted by the models is seen in experimental data for only the very deepest values of Z (> 1200 m). One possible interpretation of the problem is that some other effect not included in the models counteracts this dependence for all but the very deepest depths. Further investigation of this question must await more sophisticated models.

Because non-symmetric collapse and vertical migration broadens the bubble pulse profile as well as decreases its magnitude, the impulse is less sensitive to its effect. Consequently the models produce a better match to experimental values of bubble pulse impulse as is shown in Figures 8c and 8d. Apart from a small offset in magnitudes the models successfully match the data including the observed dependence on both *W* and Z.

5. Summary and Conclusions

Underwater explosions involve an energetic and complicated interaction between the detonating explosive and the surrounding water which can have serious consequences for any nearby structure. By virtue of their ability to couple fluid motions and target deformations FEA codes are potentially a valuable tool for studies of such events. However, before such codes can be confidently applied to the prediction of target response to a nearby detonation it must be demonstrated that they can reliably simulate experimental data for the underwater explosion itself.

As a first step in this process of verification the FEA code DYNA2D has been used to model the relatively simple case of an isolated underwater explosion producing a spherically symmetric pulsating bubble. Phenomena associated with asymmetric bubble collapse such as water jet formation were not addressed in these preliminary models. It is likely that codes incorporating a more sophisticated ALE technique or perhaps a Eulerian approach will be necessary to model these phenomena; an ALE technique will be preferred for studies involving structural response to underwater explosive loading. Despite these constraints our simplified models were able to simulate most of the important physics of an underwater explosion including the generation and propagation of shock waves, pulsation of the bubble of detonation product gases, and the generation and propagation of bubble pulse pressure waves produced by bubble collapse. Comparison to experimental results showed that the models reliably reproduced important characteristics of the explosion; values for the period and maximum diameter of the first bubble pulsation, the impulse of the shock and bubble pulse pressure waves, and the peak magnitude of the first bubble pulse were all in reasonable agreement with experimental data.

Despite these successes some problems were identified. Peak magnitudes of the shock wave were poorly reproduced due principally to the difficulty of resolving the abrupt shock front with a model of limited spatial resolution. More disappointingly characteristics of the second (and presumably subsequent) bubble pulses were also

poorly reproduced due to inadequate modelling of energy losses from the bubble. Most of this may be attributable to our assumption of spherically symmetric bubble pulsation which precludes energy losses associated with turbulence during bubble collapse. It should also be born in mind however that DYNA does not account for other potential energy loss mechanisms such as radiation from the hot bubble gases and dissolution of the bubble gases into the water. The process of non spherical pulsation can be induced in the models by specifying a non constant hydrostatic pressure gradient and this will be investigated in a subsequent paper. It is likely however that a practical approach to this problem will require the use of a more sophisticated ALE technique to handle the large element distortions encountered in non symmetric bubble collapse.

An overall objective of this study was to investigate the potential application of FEA codes such as DYNA to quantitative modelling of underwater explosive damage effects. If such codes are to be used for studies of target damage from near field events in general, then the limitations discussed above will be have to be overcome. However experimental studies show that the importance of the water jet as a damage mechanism is strongly dependent on the proximity and orientation of the explosive to the target (eg Brett et al. 1995), so that in many cases of interest the most important damage mechanisms may be loading from the shock wave and the first (and largest) bubble pulse. In these circumstances it should be possible to use DYNA2D (and presumably DYNA3D) for effective modelling of the loading from an underwater explosive event. Of course whether this produces realistic target damage will depend upon the structural model used.

6. Acknowledgents

The author would like to thank Michael Murphy for initial assistance with the FE grid and Michael Chung for useful comments on the manuscript.

7. References

Arons, A.B., Slifko, J.P. & Carter, A. 1948, Secondary pressure pulses due to gas globe oscillation in underwater explosions. I. Experimental data, *The Journal of the Acoustical Society of America,* **20,** No. 3, 475.

Arons, A.B. & Yennie, D.R. 1948, Energy partition in underwater explosion phenomena, *Reviews of Modern Physics,* **20,** No. 3, 519.

Best, J.P., & Kucera, A. 1992, A numerical investigation of non-spherical rebounding bubbles, *J. Fluid Mech.* **245,** 137.

Brett, J.M., & Reid, W.D. 1995, Modelling of target response to underwater explosions: the response of an air backed plate to near field shock loading. In: Chinni, MJ (ed). *Military, Government and Aerospace Simulation, Proceeding of the 1996 Simulation Multi-conference.*

Brett, J.M., van der Schaaf, P., & Barclay, M. 1995. An experimental study of damage to scale model cylinders from near field underwater explosions. In: *Proceedings of the 1995 Military Applications of Blast and Shock Conference.*

Chisum, J.E. & Shin, Y.S. 1996, Explosion gas bubbles near simple boundaries, *Shock and Vibration,* **4,** 11.

Cole, R.H. 1948, *Underwater Explosions,* Princeton University Press, NJ.

Coles, J.S., Christian, E.A., Slifko, F.P., Niffenegger, C.R., and Rogers, M.A. 1950 Shock wave parameters from spherical TNT charges detonated under water. In: *Underwater Explosion Research: A Compendium of British and American Reports. Vol. 1,* Office of Naval Research, Department of the Navy, Washington DC, 1085-1105.

Duncan, J.H., Milligan, C.D. & Zhang, S. 1996, On the interaction between a bubble and a submerged compliant structure, *Journal of Sound & Vibration, 197(1),* 17.

Dobratz, B.M. 1981, LLNL Explosive Handbook , UCRL-52997.

Giroux, E.D. 1973, HEMP User's Manual, University of California, LLNL Rept. UCRL-51079.

Hallquist, J.O. 1983, MAZE - An Input Generator for DYNA2D and NIKE2D. UCID 19029.

Hallquist, J.O. & Levatin, J.L., 1985, ORION: An Interactive color post-processor for two dimensional finite element codes - user manual. UCID 19310.

Huang, H. & Kiddy, K.C. 1995, Transient interaction of a spherical shell with an underwater explosion shock wave and subsequent pulsating bubble, *Shock and Vibration,* **2,** No. 6, 451.

Mader, C.L., 1971, LA4594, UC-34 TID4500.

Molyneaux, T.C.K., Li Long-Yuan & Firth, N. 1994, Numerical simulation of underwater explosions, *Computers Fluids,* **23,** No. 7, 903.

Sandusky, H., Chambers, P. and Zerilli, F. 1996, Dynamic Measurement of Plastic Deformation in a Water Filled Aluminium Tube in Response to Detonation of a Small Explosive Charge. In: *Proceedings of the 67th Shock & Vibration Symposium, Vol II,* p. 403.

Shin, Y.S. & Chisum J.E., 1996, Modeling and simulation of underwater shock problems using a coupled lagrangian - eulerian analysis approach, *Shock and Vibration,* **4,** 1.

Slifko, J.P. 1967, Pressure-Pulse Characteristics of Deep Explosions as Functions of Depth and Range, NOLTR 67-87.

Snay, H.G. 1957, Hydrodynamics of Underwater Explosions. In: *Symposium on Naval Hydrodynamics,* Publication 515. National Academy of Science, National Research Council, Washington DC, 325-352.

Swift, E. & Decius, J.C. 1950, Measurements of Bubble Pulse Phenomena, III. Radius and Period Studies. In: *Underwater Explosion Research: A Compendium of British and American Reports, Vol.* 2, Office of Naval Research, Department of the Navy, Washington, DC, 553-599.

Swisdak, M. 1978, Explosive effects and properties. II Explosive effects in water, NWSC/WOL/TR.76.116.

Whirley, R.G., Engelmann, B.E. & Hallquist, J.O., 1995, DYNA2D: A Nonlinear explicit two-dimensional finite element code for solid mechanics - user manual.

Woodruff, J.P. 1973, KOVEC user's manual, University of California, LLNL Rept. UCRL-51079.

DISTRIBUTION LIST

Numerical Modelling of Shock Wave and Pressure Pulse Generation by Underwater Explosions

John M. Brett

AUSTRALIA

DEFENCE ORGANISATION

Task Sponsor:
Director General Undersea Warfare Systems, Att. Mr P Hugonnet (Subsafe Manager)
Director General Maritime Development ,Att. Cmdr M Sanders (DDSMWD)

S&T Program

Chief Defence Scientist
FAS Science Policy
AS Science Corporate Management
} shared copy
Director General Science Policy Development
Counsellor Defence Science, London (Doc Data Sheet)
Counsellor Defence Science, Washington (Doc Data Sheet)
Scientific Adviser to MRDC Thailand (Doc Data Sheet)
Director General Scientific Advisers and Trials/Scientific Adviser Policy and Command (shared copy)
Navy Scientific Adviser
Scientific Adviser - Army (Doc Data Sheet and distribution list only)
Air Force Scientific Adviser
Director Trials

Aeronautical and Maritime Research Laboratory
Director
Chief of Maritime Platforms Division
Lincoln Wood RLMSS (MPD)
Brian Walsh
Norbert Burman
John Brett (5 copies)
David Saunders
David Ritzel
David Jones
Michael Buckland
George Yiannakopoulos
Warren Reid

DSTO Library
Library Fishermens Bend

Library Maribyrnong
Library Salisbury (2 copies)
Australian Archives
Library, MOD, Pyrmont (Doc Data sheet only)

Capability Development Division
Director General Maritime Development
Director General Land Development (Doc Data Sheet only)
Director General C3I Development (Doc Data Sheet only)

Navy
SO (Science), Director of Naval Warfare, Maritime Headquarters Annex, Garden Island, NSW 2000 (Doc Data Sheet and distribution list only)

Army
ABCA Office, G-1-34, Russell Offices, Canberra (4 copies)
SO (Science), DJFHQ(L), MILPO Enoggera, Queensland 4051 (Doc Data Sheet only)
NAPOC QWG Engineer NBCD c/- DENGRS-A, HQ Engineer Centre Liverpool Military Area, NSW 2174 (Doc Data Sheet only)

Intelligence Program
DGSTA Defence Intelligence Organisation

Corporate Support Program (libraries)
OIC TRS, Defence Regional Library, Canberra
Officer in Charge, Document Exchange Centre (DEC), 1 copy
*US Defence Technical Information Center, 2 copies
*UK Defence Research Information Centre, 2 copies
*Canada Defence Scientific Information Service, 1 copy
*NZ Defence Information Centre, 1 copy
National Library of Australia, 1 copy

UNIVERSITIES AND COLLEGES
Australian Defence Force Academy
Library
Head of Aerospace and Mechanical Engineering
Deakin University, Serials Section (M list), Deakin University Library
Senior Librarian, Hargrave Library, Monash University
Librarian, Flinders University

OTHER ORGANISATIONS
NASA (Canberra)
AGPS

OUTSIDE AUSTRALIA

ABSTRACTING AND INFORMATION ORGANISATIONS

INSPEC: Acquisitions Section Institution of Electrical Engineers
Library, Chemical Abstracts Reference Service
Engineering Societies Library, US
Materials Information, Cambridge Scientific Abstracts, US
Documents Librarian, The Center for Research Libraries, US

INFORMATION EXCHANGE AGREEMENT PARTNERS

Acquisitions Unit, Science Reference and Information Service, UK
Library - Exchange Desk, National Institute of Standards and Technology, US

SPARES (5 copies)

Total number of copies: **63**

DEFENCE SCIENCE AND TECHNOLOGY ORGANISATION
DOCUMENT CONTROL DATA

1. PRIVACY MARKING/CAVEAT (OF DOCUMENT)

2. TITLE

Numerical Modelling of Shock Wave and Pressure Pulse Generation by Underwater Explosions.

3. SECURITY CLASSIFICATION (FOR UNCLASSIFIED REPORTS THAT ARE LIMITED RELEASE USE (L) NEXT TO DOCUMENT CLASSIFICATION)

Document	(U)
Title	(U)
Abstract	(U)

4. AUTHOR(S)

John M. Brett

5. CORPORATE AUTHOR

Aeronautical and Maritime Research Laboratory
PO Box 4331
Melbourne Vic 3001 Australia

6a. DSTO NUMBER	6b. AR NUMBER	6c. TYPE OF REPORT	7. DOCUMENT DATE
DSTO-TR-0677	AR-010-558	Technical Report	June 1998

8. FILE NUMBER	9. TASK NUMBER	10. TASK SPONSOR	11. NO. OF PAGES	12. NO. OF REFERENCES
510/207/0755	NAV 97/118	DGUWS/DGMD	26	24

13. DOWNGRADING/DELIMITING INSTRUCTIONS

-

14. RELEASE AUTHORITY

Chief, Maritime Platforms Division

15. SECONDARY RELEASE STATEMENT OF THIS DOCUMENT

Approved for public release

OVERSEAS ENQUIRIES OUTSIDE STATED LIMITATIONS SHOULD BE REFERRED THROUGH DOCUMENT EXCHANGE CENTRE, DIS NETWORK OFFICE, DEPT OF DEFENCE, CAMPBELL PARK OFFICES, CANBERRA ACT 2600

16. DELIBERATE ANNOUNCEMENT

No Limitations

17. CASUAL ANNOUNCEMENT Yes

18. DEFTEST DESCRIPTORS

Underwater explosions, shock waves, detonations, bubbles, pulses, finite element analysis

19. ABSTRACT

The continuing development of multi-purpose finite element analysis (FEA) codes permits their application to provide new and penetrating insights into the difficult subject of underwater explosive effects and the coupled response of nearby structures. In this paper we investigate the use of one such code (DYNA2D) to model the physical processes associated with an underwater explosion. We compute models covering a range in explosive masses and depths of detonation. The models are shown to simulate much of the important physics of an underwater explosion including: explosive detonation, shock wave generation and transmission, bubble pulsation and the generation of bubble pulse pressure waves. The model results are compared to published experimental data for key features of an underwater explosion such as bubble periods, maximum bubble radii and characteristics of the shock and bubble pressure waves. The good quantitative agreement found for many of these features demonstrates that FEA codes can be used to model important aspects of an underwater explosion. Nevertheless a number of limitations are identified, the most serious of which is the absence of some important energy loss mechanisms associated with bubble collapse.